Mechanical strength and fracture toughness of brittle monocrystalline and ceramic materials

Marek Boniecki[1], Paweł Kamiński[1], Władysław Wesołowski[1], Konrad Krzyżak[1]

The article compares the mechanical properties of a n-type silicon single crystal with an orientation <100> and resistivity ~ 2000 Ωcm, obtained by the floating zone (FZ) method, with the mechanical properties of Y_2O_3 ceramics. Both materials are characterized by a high value of transmission coefficient of electromagnetic radiation in the wavelength range from 2 µm to 8 µm and they can be used as optical windows in a near infrared range. However, the choice of a material type for the specific applications may depend on their mechanical properties. These properties have been determined both at room temperature and at elevated temperature, i.e. 700°C for Si and 800°C for Y_2O_3 ceramics. We have found that at room temperature the fracture toughness of the Si single crystal K_{Ic} = 1.3 ± 0.1 MPam$^{1/2}$ and the four-point bending strength σ_c = 289 ± 61 MPa. For Y_2O_3 ceramics these parameters are 1.8 ± 0.2 MPam$^{1/2}$ and 184 ± 20 MPa, respectively. At 700°C the mechanical parameters for the Si single crystal are: K_{Ic} = 20 ± 3 MPam$^{1/2}$ and σ_c = 592 ± 86 MPa. For Y_2O_3 ceramics at 800°C, K_{Ic} = 1.7 ± 0.1 MPam$^{1/2}$ and σ_c = 230 ± 23 MPa. The presented data show that at elevated temperatures both fracture toughness and bending strength of the Si single crystal are significantly greater than the values of those parameters found for Y_2O_3 ceramics.

Key words: Y_2O_3 ceramics, high-purity silicon, fracture toughness, bending strength

Wytrzymałość mechaniczna i odporność na pękanie kruchych materiałów monokrystalicznych i ceramicznych

W artykule porównano właściwości mechaniczne monokrystalicznego krzemu typu n o orientacji <100> i rezystywności ~ 2000 Ωcm, otrzymanego metodą beztyglową, z właściwościami mechanicznymi ceramiki Y_2O_3. Oba materiały charakteryzują się dużym współczynnikiem transmisji promieniowania elektromagnetycznego w zakresie długości fali od 2 µm do 8 µm i mogą być stosowane jako okna optyczne w zakresie bliskiej podczerwieni. Wybór rodzaju materiału dla konkretnych zastosowań może być jednak uzależniony od ich właściwości mechanicznych. Właściwości te określano zarówno w temperaturze pokojowej, jak i w temperaturze podwyższonej do 700°C w przypadku Si oraz do 800°C w przypadku ceramiki Y_2O_3. Stwierdzono, że dla Si w temperaturze pokojowej odporność na pękanie K_{Ic} = 1,3 ± 0,1 MPam$^{1/2}$, a wytrzymałość na zginanie czteropunktowe σ_c = 289 ± 61 MPa. Dla Y_2O_3 parametry K_{Ic} i σ_c przyjmują wartości wynoszące w tej temperaturze odpowiednio 1,8 ± 0,2 MPam$^{1/2}$ i 184 ± 20 MPa. W temperaturze 700°C wartości parametrów K_{Ic} i σ_c dla Si są równe odpowiednio 20 ± 3 MPam$^{1/2}$ oraz 592 ± 86 MPa, zaś dla ceramiki Y_2O_3 w 800°C K_{Ic} = 1,7 ± 0,1 MPam$^{1/2}$ i σ_c = 230 ± 23 MPa. Prezentowane dane wskazują, że w temperaturze pokojowej wytrzymałość na zginanie czteropunktowe monokrystalicznego Si jest znacząco większa niż ceramiki Y_2O_3. W podwyższonych temperaturach zarówno odporność na pękanie, jak i wytrzymałość na zginanie monokrystalicznego Si jest wielokrotnie większa niż w przypadku ceramiki Y_2O_3.

Słowa kluczowe: ceramika Y_2O_3, krzem, odporność na pękanie, wytrzymałość na zginanie

1. Introduction

Polycrystalline ceramic materials and single crystals of semiconductors are characterized by brittle cracking. It occurs at a minimal plastic deformation, which leads to an immediate destruction of the material. This cracking usually starts from the defects already present in the material and disturb its structure. The defects can exist on the surface or in the bulk of the material. Molecules or atoms of a solid are bound together by the cohesive forces originating from the chemical or physical interactions. The cohesive strength of a material is its maximum strength, which is determi-ned by the strength of the chemical bonds and which can be theoretically estimated. In practice, such strength is rarely measured because of the aforementioned presence of numerous structural defects in the material. These defects may be microcracks, pores, inclusions of foreign phases, etc. If a load is applied to a sample made from a material containing defects, the stress concentration at the edges of these becomes many times bigger than the stress value resulting from the applied force in the defect free material. Stress concentration exeeding the material cohesive strength, result in the appearance of a crack. The cracking criterion is determined by the state of the stress field near the edges of the existing defect.

[1] *Institute of Electronic Materials Technology*, 133 Wólczynska Str., 01-919 Warsaw, Poland, e-mail: Marek.Boniecki@itme.edu.pl

The stress field is related to the shape and the size of the defect (usually understood as a crack that disturbs the continuity of the material structure) as well as to the type and the magnitude of the applied load. The analysis of that problem can be found in many textbooks and articles [1 - 4]. It presents the concept of stress intensity factor K, is proportional to the value of the applied load and depends also on the load type and the microcrack geometry. The load which is intended to destroy the material can be applied in three different ways [1, 3]. One way is called *opening* and it is a displacement perpendicular to the crack surface, while the other two (*edge slip* and *tear*) are associated with a shift parallel to the crack edge. For brittle materials (weak for stretching) the most important is the *opening* way.

It has been accepted in the literature to denote stress intensity factor corresponding to the sample destruction as K_I, which is expressed as:

$$K_I = \sigma Y \sqrt{c}, \qquad (1)$$

where: σ is the applied stress, Y is a constant dependent on the geometry of the sample and the defect (crack), while c is the crack length.

The maximum value of this factor, for the material cracking, is marked with the symbol K_{Ic} and is called fracture toughness. The value of K_{Ic} is characteristic of a given material and thus it is used to compare the mechanical properties of different materials. The destruction of a brittle material proceeds suddenly without any visible symptoms (i.e. a noticeable plastic deformation), but it is usually preceded by subcritical cracks growth. It means that under the applied stress, smaller than the critical stress (i.e. strength of the material), the initial crack present in the material starts to lengthen, reaching the critical value c_k, at which the material breaks and $K_I = K_{Ic}$. This phenomenon is described by the equation [4]:

$$V = A K_I^n, \qquad (2)$$

where: V is the propagation velocity of subcritical cracks and A and n are the parameters of the subcritical cracks growth.

The dimensions of the defects in a brittle material generated during the technological process of its production directly affect the strength σ_c of the individual samples used for the examination of their mechanical properties by a testing machine. The parameter σ_c is given by the equation:

$$\sigma_c = \frac{K_{Ic}}{Y \sqrt{c_k}}, \qquad (3)$$

The samples of a material, obtained during sintering and mechanical machining, differ in respect of the size of the defect, from which the crack growth begins and further leads to the sample destruction. Therefore, the values of the strength σ_c exhibit a particular statistical distribution. Usually this is the Weibull distribution [5], although in practice it happens to be close to the normal (Gaussian) distribution [6].

With increasing temperature, the plasticity of the material increases. It may change abruptly as in the case of a silicon single crystal, for which the temperature of the transition from a brittle to plastic state ranges from ~ 545°C to ~ 645°C, depending on the deformation rate ranging from 1.3×10^{-6} s^{-1} to 2.6×10^{-5} s^{-1} [7]. This change is accompanied by a sudden increase in the strength and fracture toughness [7]. In the case of ceramic materials, the increase in plasticity occurs gradually as a function of temperature and it does not have to be accompanied by an increase in K_{Ic} and σ_c, as it takes place e.g. in the case of Al_2O_3 ceramics [8]. On the contrary, for Y_2O_3 ceramics the values of K_{Ic} and σ_c increase or remain constant with increasing the plasticity [9 -10].

The goal of this work is to present the methodology and the results of the studies on mechanical strength, fracture toughness and subcritical crack growth for a Si single crystal of a high purity, obtained by the floating zone (FZ) method, as well as to compare our data with the previously determined mechanical properties of Y_2O_3 polycrystalline ceramics. These materials, despite their diverse microstructure, are characterized by a high value of transmission coefficient of electromagnetic radiation of the wavelength ranging from 2 μm to 8 μm and can be utilized for the production of windows transmitting the radiation in a near infrared range [11 - 12]. The comparison of the mechanical properties of these materials is very important for the selection of the type of material from the viewpoint of the requirements for the specific applications.

Mechanical properties of a Si single crystal and Y_2O_3 ceramics were examined both at room temperature and at elevated temperatures. The obtained results indicate that the measurement methods based on the theory of brittle fracture mechanics can be effectively applied to study the mechanical properties of materials of a very diversified microstructure.

2. Experimental

2.1. Samples for testing
• Si single crystal samples.

Silicon wafers mirror-like polished on one side, with a diameter of 100 mm and a thickness of 0.3 mm, were used for the tests. They were made from an n-type Si single crystal of high purity, obtained by the floating zone (FZ) method. The Si single crystal was oriented in the crystallographic direction <100> and doped with phosphorus, whose concentration was ~ 3×10^{12} cm^{-3}. The resistivity of the single crystal was ~ 2000 Ωcm. The concentration of nitrogen in the single crystal was below 3×10^{14} cm^{-3},

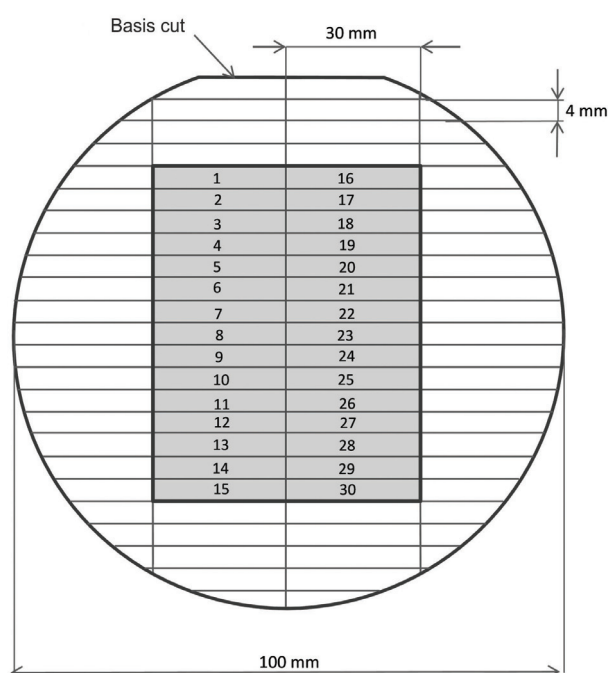Arrangement of samples on a wafer of 100 mm diameter. Orientation <100>.

Fig. 1. Arrangement of samples on a wafer made from a high-purity Si single crystal used for the tests of mechanical properties.
Rys. 1. Układ próbek na płytce z monokryształu Si o wysokiej czystości użytych do badania właściwości mechanicznych.

the concentration of oxygen was ~ 5×10^{15} cm^{-3}, and the concentration of carbon was below 5×10^{15} cm^{-3}. The silicon wafers were cut into the samples of a 4-mm width and a 30-mm length 30 mm, according to the diagram shown in Fig. 1.

• Y_2O_3 ceramics samples.

In this paper we cite the results obtained in [13 - 14] for the samples made from Y_2O_3 ceramics. A detailed description of the preparation of the ceramic samples is given in [13]. The samples used to test their mechanical properties were characterized by a density equal to 99% of the theoretical density, i.e. 5.03 g/cm^3, and by an average grain size of 6 ± 3 μm.

2.2. Tests of mechanical properties

The mechanical properties of the Si single crystal and Y_2O_3 ceramics were tested by the determination of three- and four-point bending strength, fracture toughness and Young's modulus. Three- and four-point bending strength σ_c can be expressed in the form:

$$\sigma_c = \frac{1.5P_c(L-l)}{bw^2}, \qquad (4)$$

where P_c is the fracture load, L - spacing of lower supports, l - distance of upper pressure rolls, b - sample width, and w - sample thickness.

For $l = 0$, the sample is subjected to the three-point bending. The fracture toughness K_{Ic} was determined in two ways:
(a) by three-point bending of the notched specimen,
(b) by measuring the length of the cracks propagating from the Vickers impression.

In the case of the method (a), the value of K_{Ic} was calculated from the formula:

$$K_{Ic} = Y \frac{1.5P_c L}{bw^2} c_k^{0.5}, \qquad (5)$$

where Y is a geometrical constant calculated according to the description given in [15], c_k – the notch depth, while the remaining designations are as defined above.

For the method (b), K_{Ic} was calculated from the formula [16]:

$$K_{Ic} = 0.016 (E/H)^{0.5} (P/c^{1.5}), \qquad (6)$$

where E is elastic (Young's) modulus, H - Vickers hardness, P - load of the Vickers indenter, c - length of the cracks propagating from the corners of the impression.

A more detailed discussion on the ways of K_{Ic} measurements with the use of Vickers indenter can be found in [14].

The value of Young's modulus E was determined by the three-point bending method and calculated from the formula [15]:

$$E = \frac{L^2}{bw^2c} \left[\frac{L}{4w} + \frac{(1+v)w}{2L} \right], \qquad (7)$$

where $C = \Delta y/\Delta P$ denotes the ratio of the increase in the sample deflection to the load increase, v is the Poisson constant, while the remaining designations are as defined above.

The hardness H was determined from the measurements of the diagonal length of the Vickers impression. The value of H was calculated from the formula:

$$H = 1.8544 \times P/(2a)^2, \qquad (8)$$

where a is the half-length of the diagonal of the Vickers impression and P is the load of the Vickers indenter.

3. Results

A comparison of strength characteristics for the Si single crystal and for Y_2O_3 ceramics is presented in Fig. 2 in the form of diagrams of the two-parametric Weibull distribution. The tests were carried out at the loading head travelling speed of 1 mm/min at room temperature as well as at 700ºC for Si and 800°C for Y_2O_3. The measurements of σ_c for a Si single crystal were performed in a four-point

bending system using the samples with a thickness of 0.3 mm, shown in Fig. 1. The distance between the bottom supports was 20 mm, while between the upper supports it was 10 mm (the stretched surface was polished). In the case of Y_2O_3 ceramics, the sample width was 0.95 mm, thickness 1 mm and length 15 mm. The measurements of σ_c were performed in a three-point bending system with the distance between the supports equal to 8 mm.

The cumulative distribution function of two-parameter Weibull distribution is represented by the formula [5]:

$$P = 1 - \exp\left[-\left(\frac{\sigma_c}{\sigma_0}\right)^m\right], \qquad (9)$$

where P denotes the probability of sample destruction under stress σ_c, σ_0 - the characteristic stress and m – the Weibull module (distribution shape parameter).

In the coordinate system where the values of $\ln(\sigma_c)$ are on the X-axis and the values of $\ln(\ln(1/(1 - P)))$ are on the Y-axis, the experimental points should follow a straight line, on which to a point at a position i (the points are put with ascending strength values) the probability of a destruction given by the equation (10) [6] is assigned:

$$P = \frac{i - 0.5}{N}, \qquad (10)$$
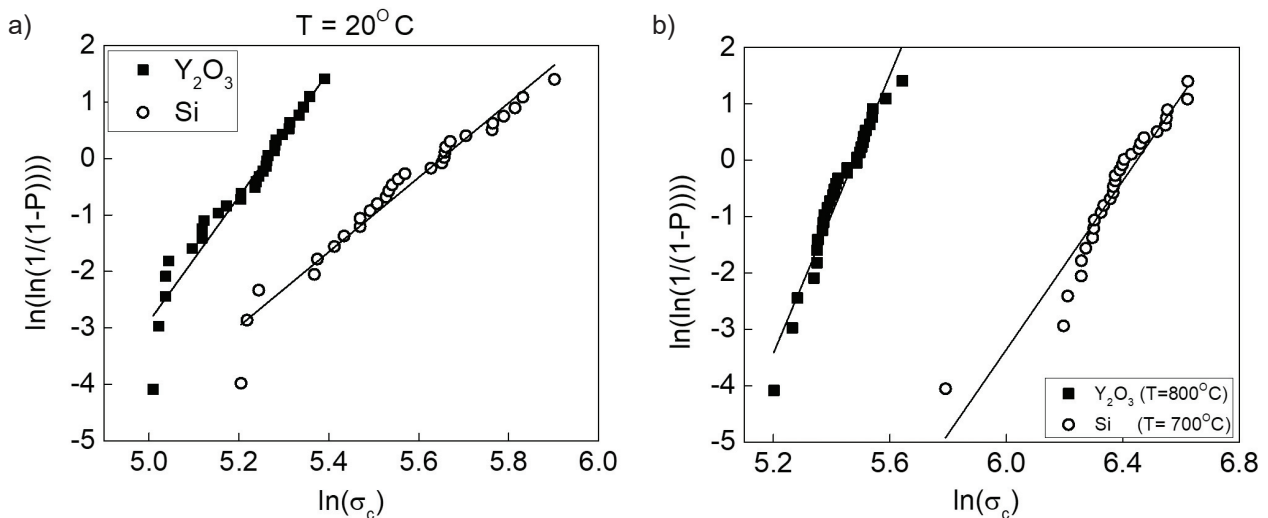
where N is the number of samples.

Fig. 2. Comparison of the Weibull distribution plots for the strength of the Si single crystal (wafer No. 4, Tab. 1) and Y_2O_3 ceramics: (a) at room temperature, (b) at elevated temperature (700ºC for Si and 800ºC for Y_2O_3 [13]).
Rys. 2. Porównanie wykresów rozkładu Weibulla wytrzymałości monokrystalicznego Si (płytka nr 4, Tab. 1) i ceramiki Y_2O_3: (a) w temperaturze pokojowej, (b) w temperaturze podwyższonej (700ºC dla Si i 800ºC dla Y_2O_3 [13]).

Tab. 1. Gaussian and Weibull distribution parameters of the Si wafers strength at $T = 20ºC$.
Tab. 1. Parametry rozkładów Gaussa i Weibulla dla wytrzymałości płytek Si w temperaturze 20ºC.

Wafer number	min (MPa)	max (MPa)	Gaussian distribution		Weibull distribution					N
			S (MPa)	O (MPa)	m	σ_o (MPa)	E_0 (MPa)	$\sigma_{0.5}$ (MPa)	W (MPa)	
1	129.7	314.5	202.0	47.5	5.08	219.2	201.2	203.9	46.5	24
2	152.1	476.3	300.2	92.0	3.73	335.7	303.0	304.3	91.1	29
3	148.3	428.3	309.5	77.5	4.34	341.8	312.0	314.1	77.8	30
4	197.1	438.8	343.7	59.8	6.44	369.4	343.5	349.0	65.5	30
Mean			**288.9**	**69.2**	**4.89**	**316.5**	**289.9**	**292.8**	**70.2**	

The symbols *min* and *max* denote the minimal and maximal measurement result respectively, N - the number of measurements. The Gaussian distribution parameters: arithmetic mean S and standard deviation O. The Weibull distribution parameters: expected value $E_0 = \sigma_u + \sigma_0 \Gamma(1 + 1/m)$, variance square root $W = \sigma_0 \{\Gamma(1 + 2/m) - \Gamma^2(1 + 1/m)\}^{1/2}$, and median $\sigma_0 = \sigma_0 \ln(2)^{1/m}$ (Γ is Euler's gamma function).

Tab. 2. Gaussian and Weibull distribution parameters for the strength of Y_2O_3 ceramics at 20ºC [13].
Tab. 2. Parametry rozkładów Gaussa i Weibulla dla wytrzymałości ceramiki Y_2O_3 w temperaturze 20ºC [13].

min (MPa)	max (MPa)	Gaussian distribution		Weibull distribution					N
		S (MPa)	O (MPa)	m	σ_o (MPa)	E_0 (MPa)	$\sigma_{0.5}$ (MPa)	W (MPa)	
149.8	220.0	184.3	20	11.1	193.0	184.4	186.7	20.0	30

Tab. 3. Gaussian and Weibull distribution parameters for the strength of Si wafers and Y_2O_3 [13] ceramics at temperatures 700ºC and 800 ºC, respectively.
Tab. 3. Parametry rozkładów Gaussa i Weibulla wytrzymałości płytek Si i ceramiki Y_2O_3 [13] w temperaturach odpowiednio 700ºC i 800ºC.

Material	min (MPa)	max (MPa)	Gaussian distribution		Weibull distribution					N
			S (MPa)	O (MPa)	m	σ_o (MPa)	E_0 (MPa)	$\sigma_{0,5}$ (MPa)	W (MPa)	
Si	327.5	752.1	592.4	85.7	8.88	627.3	594.0	601.6	94.6	29
Y_2O_3	181.6	282.3	229.8	22.7	10.90	240.0	229.1	232.1	25.4	30

Tab. 1 and 2 present the calculated values of the Weibull distribution parameters derived from the plots in Fig. 2 (a) for the Si single crystal and Y_2O_3 ceramics at 20ºC, respectively. The comparison is also presented for the values of the arithmetic mean S and standard deviation O (Gaussian distribution) determined from our experimental data with the expected value E, median $\sigma_{0.5}$ and variance square root W, calculated from Weibull distribution parameters for Si and Y_2O_3 ceramics at room temperature, respectively. The strength tests of Si were carried out using the samples made from four different wafers (Tab. 1) originating from one single crystal. Tab. 3 shows the comparison of the Weibull and Gaussian distributions parameters for the Si crystal at 700ºC and Y_2O_3 ceramics at 800ºC, respectively.

Tab. 4 and 5 collect the values of K_{Ic}, E and H, determined for the Si single crystal and Y_2O_3 ceramics, respectively. Each number given in the tables is the value of an arithmetic mean for five samples.

The values of K_{Ic} and H shown in Tab. 4 were determined using the Vickers indenter at a load P = 4.9 N. The K_{Ic} values were calculated from the formula (6), while the H values was were obtained by applying the equation (8). The samples shown in Fig. 1 and the three-point bending method with a support distance of 25 mm were used to determine the Young's modulus E. The E values were determined from the formula (7), assuming v = 0.28. It is worth adding that the fracture toughness K_{Ic} for the Si wafers determined using the notched bar samples was 1.3 ± 0.1 MPam$^{1/2}$. The measurements were carried out on the samples as shown in Fig. 1 with the notch cut in the distance of ~ 1 mm from the edge of the specimen with the support beams spacing of 20 mm.

The K_{Ic} (Vickers) and H values were determined using a Vickers indenter at a load P = 98.1 N. The E values were

Tab. 4. Fracture toughness K_{Ic}, Young's modus E and Vickers hardness H for the Sisingle crystal at room temperature 20ºC.
Tab. 4. Odporność na pękanie K_{Ic}, moduł Younga E oraz twardość Vickersa H dla monokrystalicznego krzemu w temperaturze 20ºC.

Wafer number	K_{Ic} (MPam$^{1/2}$)	E (GPa)	H (GPa)
1	0.73 ± 0.07	161 ± 14	9.9 ± 0.8
2	0.79 ± 0.06	172 ± 10	9.6
3	0.78 ± 0.08	178 ± 10	10 ± 1
4	0.70 ± 0.04	180 ± 9	9.8 ± 0.4
Mean	**0.75 ± 0.04**	**173 ± 9**	**9.9 ± 0.2**

Tab. 5. Facture toughness K_{Ic}, Young's modus E and Vickers hardness H for Y_2O_3 ceramics at 20ºC [14].
Tab. 5. Odporność na pękanie K_{Ic}, moduł Younga E oraz twardość Vickersa H dla ceramiki Y_2O_3 w temperaturze 20ºC [14].

K_{Ic} (MPam$^{1/2}$)		E (GPa)	H (GPa)
beam	Vickers		
1.8 ± 0.2	1.0 ± 0.1	158 ± 8	7.5 ± 0.2

obtained using the samples in the form of notched beams 1 mm thick, 4 mm wide and 50 mm long, by applying the three-point bending method with the support beams spacing of 40 mm. The values were calculated according to the formula (7), assuming v = 0.3. The K_{Ic} value (beam) was determined using beam-shaped samples with a thickness of w = 4 mm, width b = 2.5 mm, length l = 30 mm,

and with the notch depth c_k = 1.1 mm, by applying the three-point bending method with the support beams spacing L = 20 mm.

It should be added that the fracture toughness K_{Ic}, measured with the use of the samples in the form of notched beams was 19.9 ± 2.6 and 1.7 ± 0.1 MPam$^{1/2}$ for the Si single crystal at 700ºC and Y$_2$O$_3$ ceramics at 800ºC, respectively [13].

When comparing the results for Si and Y$_2$O$_3$, it is necessary to comment on the reliability of the values of K_{Ic} obtained by the bending method for the notched beams, in particular for the Si wafers. In the case of the Si samples, the ratio of the transverse dimensions of the samples w/b = 4/0.3 = 13.3, while for Y$_2$O$_3$ $_{w/b}$ = 4/2.5 = 1.6. However, the formula taken from [15] and used for the calculations of K_{Ic} can be applied to all cases if the single condition $L/w \geq 2$ is fulfilled. A high w/b value for the Si samples can lead to erroneous K_{Ic} results due to a different distribution of stresses in the samples that deviate far from the standard dimensions (for w/b ranging from 1 to 4, according to an ASTM E-399-90 standard). Unfortunately, since only the 0.3 mm thick Si wafers were available to the authors, it was not technically possible to produce samples meeting the condition $1 \leq w/b \leq 4$. It should also be stressed that the notches on Si and Y$_2$O$_3$ samples were performed by the same technique (cutting up to a depth of 0.8 mm with the use of a 0.2 mm wide disc, and up to around 1 mm with the use of a 0.05 mm wide disc). The spacing between supports was 20 mm in both cases.

Among many methods of the measurement of the values of the subcritical crack growth parameters A and n (formula (2)), we have chosen the measurement of the bending strength of the beams as a function of the load application rate [17]. On the basis of the formulas (1) and (2), the following relationship has been derived in [17] between the strength σ_f for a given loading rate and the loading rate $d\sigma/dt$, expressed in the logarithmic form as:

$$\log \sigma_f = \frac{1}{n+1} \log (d\sigma/dt) + \frac{1}{n+1} \log [B(n+1)\sigma_c^{n-2}], \quad (11)$$

where: $B = 2/[(n-2)AY^2 K_{Ic}^{n-2}]$.

In the coordinate system where the values of log $(d\sigma/dt)$ are on the X-axis and the values of log (σ_f) are on the Y-axis, the experimental points follow a straight line. Fig. 3 presents a comparison of the results obtained at room temperature for the Si single crystal and Y$_2$O$_3$ ceramics. The strength measurements were carried out for four displacement rates of the testing machine head: 0.001, 0.01, 0.1 and 1 mm/min. The corresponding rates of the load increase were determined on the basis of a digital recording of the force as a function of time. All the experimental points shown in Fig. 3 are averaged over 10 measurements. The parameters of the equation (11) were calculated using the least squares method, and then the values A and n (Tab. 6)

Tab. 6. Parameters of the equation (2) describing subcritical crack growth, determined for the Si single crystal and Y$_2$O$_3$ ceramics.

Material Parameter	Si	Y$_2$O$_3$
n	75.2	51.7
A (m/s)	1.8×10^{-15}	4.8×10^{-19}

The parameters n and A for Y$_2$O$_3$ ceramics were calculated on the basis of the experimental data given in [13].
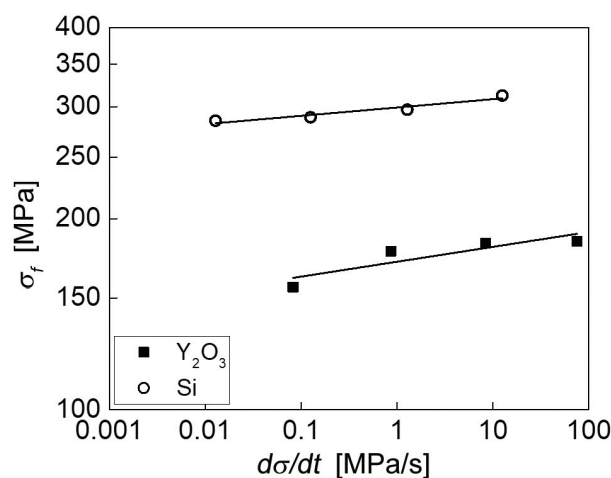

Fig. 3. Comparison of bending strength σ_f as a function of loading rate $d\sigma/dt$ for the Si single crystal and Y$_2$O$_3$ ceramics at room temperature.
Rys. 3. Porównanie wytrzymałości na zginanie σ_f w funkcji szybkości obciążania $d\sigma/dt$ dla monokrystalicznego Si i ceramiki Y$_2$O$_3$ w temperaturze pokojowej.

were obtained using the following values in the calculations σ_c and K_{Ic}: 288.9 MPa (a mean S value from Tab. 1), 184.3 MPa (S value from Tab. 2), 1.3 MPam$^{1/2}$ and 1.8 MPam$^{1/2}$ for the Si wafers and Y$_2$O$_3$ ceramics, respectively. The value of σ_c for the Si wafers corresponds to the strength measured for the load application rate of 1 mm/min, while for Y$_2$O$_3$ it is the value of parameter S from Tab. 2. The K_{Ic} values were measured on the notched beams (Tab. 4 and 5) and Y was taken from the work [3] as equal to $\sqrt{\pi}$ (1.8).

4. Discussion of the results

4.1. Comparison of mechanical properties of Si wafers and Y$_2$O$_3$ ceramics at room temperature

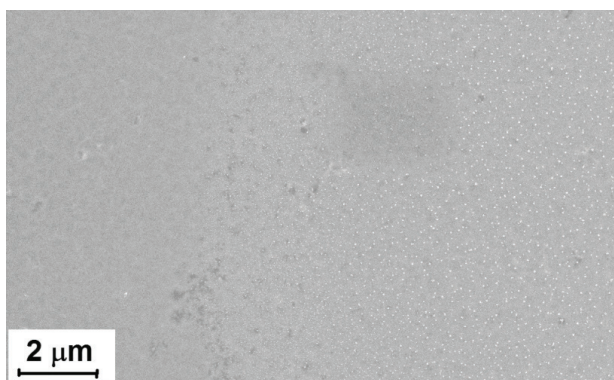In the work [18], the bending strength of Si wafers (diameter ~ 76 mm and thickness 0.69 mm) was

Fig. 4. Microscopic image of the etched surface of a Si wafer.
Rys. 4. Mikroskopowy obraz powierzchni płytki Si po wytrawieniu.

tested and the results depended on the method of the preparation of the wafer stretched surface. The samples originated from <111> single crystals were obtained by the FZ method. No nitrogen was detected in these samples, while the concentration of oxygen was comparable to the samples used in our study and it amounted to ~ 4×10^{15} cm^{-3}. For the Si wafers with a non-polished surface the mean strength value equalled ~ 220 MPa and the value of Weibull module $m = 16.2$ indicated a small scatter of the results. On the other hand, for the polished samples, the average strength value was ~ 1.1 GPa, but there was a large scatter of results ($m = 3$). When comparing these results with the data listed in Tab. 1, in the case of our study the observed difference can be due to a significant influence of the edge faults, which probably do not play a role in the load geometry used in [18]. This fact may signify that the mean strength of the polished Si samples in our work is slightly higher than that of the non-polished ones in [18], but at the same time the scatter of the test results is large. For Y$_2$O$_3$, the value of $m = 11.1$ indicates that the scatter of the results is smaller than in the case of Si wafers, even though the ceramic samples were not polished. In [19] for the non-polished Al$_2$O$_3$ ceramic samples the value of parameter m was also ~ 11 (the samples were tested for three-point bending). The analysis of the defects size, resulting from the dependence (3), shows that for the Si wafers the value of critical defect $c_k \approx 6$ μm ($K_{Ic} = 1.3$ MPam$^{1/2}$ from Tab. 4, $\sigma_c = 288.9$ MPa from Tab. 1, $Y = 1.8$), while for Y$_2$O$_3$ ceramics $c_k \approx 30$ μm ($K_{Ic} = 1.8$ MPam$^{1/2}$ from Tab. 5, $\sigma_c = 184.3$ MPa from Tab. 2).

As mentioned in the Introduction, the defects in the material may be of various form e.g. grain boundaries, microcracks, pores or inclusions of foreign phases. Defects of this kind are commonly present in the ceramic materials, but they do not exist in a pure Si single crystal. According to the literature reports [20], the so-called oxygen precipitates (the regions where inclusions of SiO$_x$ compounds are present) occur in Si. They may have a size from several nm to dozens of nm, while their concentration in the bulk may reach ~ 1×10^9 cm^{-3} [21]. Of course,

the dimensions of these defects are much smaller than those calculated above, i.e. 6 μm, but when ones takes into account the value of $\sigma_c = 1.1$ GPa from [18], then $c_k \approx 0.4$ μm, which is much closer to the observed precipitate size. Fig. 4 presents a scanning electron microscopic image of the chemically etched surface of the FZ Si sample, where the etched holes are visible as white spots, indicating the possible presence of oxygen precipitates.

The mechanical properties of Si are anisotropic [22] and the cracking energy depends on a given crystallographic plane. Therefore, the fracture toughness K_{Ic} also depends on the crystallographic orientation of the tested sample [22 - 23]. The results of the tests presented in [23] indicate that for the plane (001) K_{Ic} ranges from 0.75 to 1.29 MPam$^{1/2}$. This scatter of the results is mainly due to the use of different research methods. As evidenced by the data presented in Tab. 4, the K_{Ic} value measured by the Vickers method is 0.75 MPam$^{1/2}$, while the K_{Ic} value obtained by the notched beam method is 1.3 MPam$^{1/2}$. The values of the Young's modulus E ranges from 130 to 190 GPa, depending on the crystallographic direction [22 - 23], while the hardness H ranges from 11 - 16 GPa [22]. In Tab. 4, the values of E and H are 173 and 9.9 GPa, respectively. The mechanical properties of the Si single crystal compare favorably with those of Y$_2$O$_3$ ceramics. The values of the mechanical parameters other than the fracture toughness are higher for this crystal than those for Y$_2$O$_3$ ceramics. However, it should be noted here that other ceramic materials possess better mechanical properties than Y$_2$O$_3$ ceramics. For instance, Al$_2$O$_3$ ceramics is characterized by the following parameters [24]: $\sigma_c = 413 \pm 43$ MPa, $K_{Ic} = 5.0 \pm 0.4$ MPam$^{1/2}$, $E = 380$ GPa, and $H = 15 \pm 2$ GPa [8]. On the other hand, for the composite 20% Al$_2$O$_3$ - 80% ZrO$_2$ [25]: $\sigma_c = 1500 \pm 260$ MPa, $K_{Ic} = 5.5 \pm 0.3$ MPam$^{1/2}$, $E = 235 \pm 12$ GPa, $H = 15{,}0$ GPa.

The values of subcritical crack growth parameter n, shown in Tab. 6 for Y$_2$O$_3$ ceramics, are close to the values obtained by the same method for other ceramic materials, e.g. for Al$_2$O$_3$ and Al$_2$O$_3$ - ZrO$_2$ ceramics [24]. However, the value of $n = 75.2$ for Si is significantly higher than the value of n parameter for the ceramic materials. This fact indicates that the propagation of cracks proceeds here in a narrow range of K_I values, close to the values of K_{Ic}. It can be concluded that, compared to the ceramics, monocrystalline Si is a material more resistant to subcritical cracks growth.

4.2. Comparison of mechanical properties of Si wafers and Y$_2$O$_3$ ceramics at elevated temperatures

The obtained results indicate that at 700°C the bending strength of the Si wafers increases more than twice (an increase by 105%). In other words, the material becomes more plastic, as shown in Fig. 5. which means that the destruction of the sample is preceded by the plastic deformation. As shown by the results of the tests presented in [7], at 700°C monocrystalline Si can undergo a deformation due to the generation of dislocations.

The tests of our work proved [7] that the temperature of a Si single crystal transition from a brittle to plastic state at a deformation rate of 2.6×10^{-5} s^{-1} equals ~ 660°C. The tests were carried out at 700°C with a deformation rate of ~ 5.6 ± 10^{-5} s^{-1}. It should be added that the temperature of this transition increases as a function of deformation rate and depends on the content of the dopants and impurities present in Si single crystals. It was observed that during the cracking the silicon samples disintegrated into a dozen of even dozens of small pieces (while usually into no more than two pieces at room temperature). On the other hand, the K_{Ic} values (measured on a notched bar) are approximately 15 times greater at 700°C than at 20°C. This fact confirms the thesis on the change in the nature of cracking from brittle to plastic. Due to this change, the value of the Weibull modulus increased from $m = 4.9$ (Tab. 1) at room temperature to 8.9 (Tab. 3) at 700°C which resulted in a significant reduction in the scatter of the obtained experimental results.

Based on the available literature data [26], the mechanism of cracking of silicon samples at 700°C can be proposed as follow. In these samples, the mobile dislocations are generated at 700°C and when the external force becomes increased the length of their displacement path increases too. However, the clusters of oxygen atoms or SiO$_x$ phase precipitations that are present in the material block the dislocation movement. As a result of the dislocation motion blocking, a large stress may arise in many areas of the Si wafer leading to the cleavage of covalent bonds between the neighboring Si atoms. The continuity of the crystal structure of the material gets broken, which is manifested by the disintegration of the wafer into many small pieces.

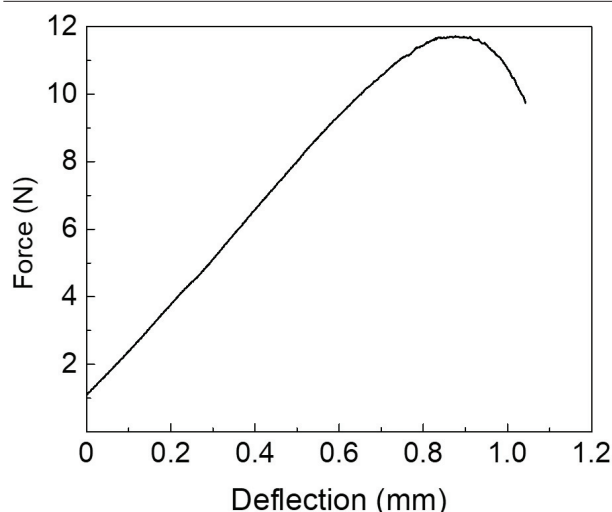In the case of Y$_2$O$_3$ ceramics, the plastic deformation of the material does not occur and cracking at 800°C is still brittle. The values of K_{Ic} parameter does not change, while bending strength of the material increases by ~ 25% in comparison with the strength measured at room temperature. This increase can be explained by a change in the mechanism of the material cracking. At room temperature, cracking takes place mainly inside the grains. At 800°C, the dominant mechanism of the material destruction is cracking at grain boundaries [10].

The analysis of the mechanical properties of a the Si single crystal and Y$_2$O$_3$ ceramics at elevated temperatures leads to the conclusion that monocrystalline Si seems to be a better constructional material as compared not only with Y$_2$O$_3$ ceramics, but also with other ceramic materials. First of all, it is characterized by a much greater fracture toughness than ceramic materials. The value of K_{Ic} parameter determined in this paper equals ~ 20 MPam$^{1/2}$. It is also noteworthy that the high value of bending strength for the Si single crystal reaches 600 MPa, which is significantly higher than that for Al$_2$O$_3$, i.e. ~ 413 MPa [24].

5. Summary

This paper presents the results of investigations of the mechanical properties of Si wafers made from the high-purity Si single crystal obtained by the floating zone (FZ) method. The values of bending strength, fracture toughness, the Young's modulus and material hardness have been determined. The samples were prepared from an n-type silicon single crystal with a crystal orientation <100> and resistivity ~ 2000 Ωcm. The concentration of phosphorus in the Si single crystal was ~ 3×10^{12} cm^{-3} and the concentration of interstitial oxygen atoms was equal to ~ 5×10^{15} cm^{-3}. The bending strength and fracture toughness were determined at both 20°C and 700°C. The mechanical properties of the Si wafers were compared with the properties previously determined for Y$_2$O$_3$ ceramics at 20°C and 800°C. Both materials can be used for the production of windows transmitting infrared radiation with the wavelength ranging from 2 μm to 8 μm and the choice of the material for the specific applications may depend on its mechanical properties. It has been found that at room temperature, the fracture toughness of monocrystalline Si is smaller than that of Y$_2$O$_3$ ceramics. At the same time, bending strength of the Si single crystal is greater than that of the ceramic material. Based on the literature reports, we have presented a mechanism indicating that the clusters of oxygen atoms or SiO$_x$ precipitates are those defects in the structure of Si, from which the critical crack can start to propagate. At 700°C, monocrystalline Si undergoes the plastic deformation and the dislocations are generated in the material, accompanied by an abrupt increase in the values of the fracture toughness and strength. Fracture toughness and bending strength of the monocrystalline

Fig. 5. Relationship between deflection and load, determined during the bending test of a the monocrystalline Si beam at 700°C.
Rys. 5. Krzywa ugięcie-obciążenie, wyznaczona w próbie zginania belki monokrystalicznego Si w temperaturze 700°C.

silicon at temperatures above the temperature of transition from brittle-to-plastic state are probably dependent on the dislocation mobility, and the movement within the crystal may be blocked by the clusters of oxygen atoms or SiO_x inclusions.

Acknowledgements

References

[1] Ranachowski J.: Elektroceramika: Własności i nowoczesne metody badań, Warszawa – Poznań, PWN, 1981

[2] Guy A. G.: Wprowadzenie do nauki o materiałach, Warszawa, PWN, 1977

[3] Thomson R. M.: Physics of fracture, *J.Phys.Chem. Sol.,* 1987, 48 (11), 965 – 983

[4] Freiman S. W.: Brittle fracture behaviour of ceramics, *Ceram. Bull.,* 1988 , 67(2), 392 – 402

[5] Rećko W. M.: O module Weibulla – historia i przyszłość, *Ceramika/Ceramics,* 2003, 80, 253 – 258

[6] Rećko W. M.: Rozkład Weibulla dla wytrzymałości na ściskanie, *Szkło i Ceramika,* 2008, 59, 2 – 5

[7] Samuels J., Roberts S. G.: The brittle-ductile transition in silicon. I. Experiments, *Proc. R. Soc. London, Ser. A,* 1989, 421, 1 – 23

[8] Munro R. G.: Evaluated material properties for a sintered α-alumina, *J. Am. Ceram. Soc.,* 1997, 80(8), 1919 – 1928

[9] Desmaison-Brut M., Montintin J., Valin E., Boncoeur M.: Influence of processing conditions on the microstructure and mechanical properties of sintered yttrium oxides, *J. Am. Ceram. Soc.,* 1995, 78(3), 716 – 722

[10] Boniecki M., Librant Z., Wesołowski W. et al.: Fracture mechanics of Y_2O_3 ceramics at high temperatures, *Advances in Science and Technology,* 2014, 89, 88 – 93

[11] Nigara Y.: Measurement of optical constants of yttrium oxide, *Jpn. J. Appl. Phys.,* 1968, 7, 404 – 408

[12] Harris Daniel C.: Materials for infrared windows and domes: properties and performance, SPIE – The International Society for Optical Engineering, Bellingham, Washington 1999, 150 – 191

[13] Boniecki M., Jach K., Librant Z., et al.: Mechanika kruchego pękania ceramiki Y_2O_3, *Materiały Ceramiczne/Ceramic Materials,* 2015, 67, 1, 43 – 47

[14] Boniecki M., Librant Z., Wesołowski W. et al.: Odporność na pękanie ceramiki Y_2O_3, *Materiały Ceramiczne/Ceramic Materials,* 2015, 67, 4, 378 – 382

[15] Fett T., Munz, D.: Subcritical crack growth of macrocracks in alumina with R-curve behavior, *J. Am. Ceram. Soc.,* 1992, 75, 4, 958 – 963

[16] Anstis G. R., Chantikul P., Lawn B. R., Marshall D. B.: A critical evaluation of indentation techniques for measuring fracture toughness: I. Direct crack measurements, *J. Am. Ceram. Soc.,* 1981, 64, 9, 533 – 538

[17] Wiederhorn S. M.: Subcritical crack growth in ceramics, Fracture Mechanics of Ceramics v.2, ed. by Bradt R.C., Hasselman D. P. H., Lange F. F., New York, London, Plenum Press, 1974, 613 – 646

[18] Vedde J., Gravesen P.: The fracture strength of nitrogen doped silicon wafers, *Mater. Sci. Eng.,* 1996, B36, 246 – 250

[19] Dziubak C., Rećko W. M.: Statystyka wytrzymałości ceramiki korundowej, *Szkło i Ceramika,* 2009, 60, 7 – 11

[20] Zeng Y., Ma X., Chen J., Yang D.: Correlation between oxygen precipitation and extended defects in Czochralski silicon: Investigation by means of scanning infrared microscopy, *J. Electronic. Mater.* 2010, 39 (8), 648 – 651

[21] Achmetov V. D., Richter H., Lysytskiy O., Wahlich R., Muller T.: Oxide precipitates in annealed nitrogen-doped 300 mm CZ-Si, *Mater.Sci. Semiconductor Processing,* 2003, 5, 391 – 396

[22] Ebrahimi F., Kalwani L.: Fracture anisotropy in silicon single crystal, *Mater. Sci. Eng.* 1999, A268, 116 – 126.

[23] Masolin A., Bouchard P. O., Martini R., Bernacki M.: Thermo-mechanical and fracture properties in single--crystal silicon, *J. Mater. Sci.* 2013, 48, 979 – 988

[24] Boniecki M.: Wpływ mikrostruktury na rozwój mikropęknięć podkrytycznych w materiałach ceramicznych, *Materiały Elektroniczne – Electronic Materials,* 1992, 1 (77), 8 – 29

[25] Boniecki M., Gołębiewski P., Wesołowski W., et al.: Kompozyt Al_2O_3 – ZrO_2 wzmocniony płatkami grafenowymi, *Materiały Elektroniczne – Electronic Materials,* 2016, 44, 1, 20 – 28

[26] Hu S. M.: Dislocation pinning effect of oxygen atoms in silicon, *Apl. Phys. Lett.* 1977, 31 (2), 53 – 55